Dalton Transactions

ROYAL SOCIETY OF CHEMISTRY

PAPER

View Article Online
View Journal | View Issue

Cite this: *Dalton Trans.*, 2023, **52**, 9090

Catalytic activation of remote alkenes through silyl-rhodium(III) complexes†

Unai Prieto-Pascual,[a] Aitor Martínez de Morentin,[a] Duane Choquesillo-Lazarte,[b] Antonio Rodríguez-Diéguez,[c] Zoraida Freixa *[a,d] and Miguel A. Huertos *[a,d]

Received 28th February 2023,
Accepted 30th May 2023

DOI: 10.1039/d3dt00624g

rsc.li/dalton

The tandem isomerization–hydrosilylation reaction is a highly valuable process able to transform mixtures of internal olefins into linear silanes. Unsaturated and cationic hydrido-silyl-Rh(III) complexes have proven to be effective catalysts for this reaction. Herein, three silicon-based bidentate ligands, 8-(dimethylsilyl) quinoline (**L1**), 8-(dimethylsilyl)-2-methylquinoline (**L2**) and 4-(dimethylsilyl)-9-phenylacridine (**L3**), have been used to synthesize three neutral [RhCl(H)(**L**)PPh_3] (**1-L1**, **1-L2** and **1-L3**) and three cationic [Rh(H)(**L**)$(PPh_3)_2$][$BAr^F{}_4$] (**2-L1**, **2-L2** and **2-L3**) Rh(III) complexes. Among the neutral compounds, **1-L2** could be characterized in the solid state by X-ray diffraction showing a distorted trigonal bipyramidal structure. Neutral complexes (**1-L1**, **1-L2** and **1-L3**) failed to catalyze the hydrosilylation of olefins. On the other hand, the cationic compound **2-L2** was also characterized by X-ray diffraction showing a square pyramidal structure. The unsaturated and cationic Rh(III) complexes **2-L1**, **2-L2** and **2-L3** showed significant catalytic activity in the hydrosilylation of remote alkenes, with the most sterically hindered (**2-L2**) being the most active one.

Introduction

Alkylsilanes are important academic and industrial feedstocks because they are valuable precursors for silicon-based polymers, lubricants and water-repellent coatings, among others.[1–3] Focusing on linear alkylsilanes, their common synthesis is through the hydrosilylation of terminal alkenes using platinum catalysts, such as Speier's[4,5] and Karstedt's catalysts.[6] During the last few decades, the hydrosilylation of carbon–carbon multiple bonds catalyzed by first-row transition metal compounds has been extensively studied.[7–15] The problem with such systems is that high temperatures are required, resulting in the formation of undesirable side products.[16] The use of some iron complexes has mitigated this problem.[17–19] However, the catalytic systems discussed above have a limitation, which is the necessity of using terminal olefins (α-olefins) to obtain linear alkylsilanes.[20]

The industrial production of α-olefins is mainly carried out by using two processes, oligomerization of ethylene and cracking/reforming of oil. In both cases, the final product is a mixture of terminal and internal olefins. For this reason, it is economically attractive to find methods that valorize this mixture of internal and terminal olefins. One of these methods is the catalytic isomerization–functionalization of these mixtures. In recent years, promising results using cobalt,[21] nickel,[22] iron[23] and rhodium[24–27] complexes as homogeneous catalysts for tandem isomerization–hydrosilylation have been reported (Fig. 1).

Focusing on rhodium complexes, in 1970 Chalk reported that Wilkinson's catalyst was able to catalyze the tandem isomerization–hydrosilylation reaction to obtain dimethyl(pentyl)(phenyl)silane (20% yield) from *cis*-2-pentene and dimethyl(phenyl)silane.[28] In the same work, hydrido-silyl-Rh(III) intermediates[29] were suggested to be involved in the isomerization reaction. For this reason, in earlier reports, we considered synthesizing hydrido-silyl-Rh(III) complexes and using them as catalysts in the isomerization–hydrosilylation tandem reaction. In 2017, we reported a rhodium silyl complex containing a Si, S-chelating ligand, [Rh(H){$SiMe_2$(*o*-C_6H_4SMe)}$(PPh_3)_2$][$BAr^F{}_4$], as a very efficient catalyst for tandem isomerization–hydrosilylation from internal alkenes to linear silanes under mild reaction conditions (Fig. 1).[24] Most recently, in 2021, we expanded the scope of hydrido-silyl-Rh(III) complexes through the synthesis of bidentate Si,S ligands with different substituents on the sulfur atom [$SiMe_2$H(*o*-C_6H_4SR)] (R = ^{i}Bu, pentyl, benzyl,

[a]*Facultad de Química, Universidad del País Vasco (UPV/EHU), 20018 San Sebastián, Spain. E-mail: miguelangel.huertos@ehu.es, Zoraida_freixa@ehu.eus*
[b]*Laboratorio de Estudios Cristalográficos, IACT, CSIC-UGR, 18071 Granada, Spain*
[c]*Dpto. Química Inorgánica, Universidad de Granada, 18071 Granada, Spain*
[d]*IKERBASQUE, Basque Fundation for Science, 48011 Bilbao, Spain*

†Electronic supplementary information (ESI) available: Spectroscopic characterization and crystallography studies. CCDC 2219493 and 2219494. For ESI and crystallographic data in CIF or other electronic format see DOI: https://doi.org/10.1039/d3dt00624g

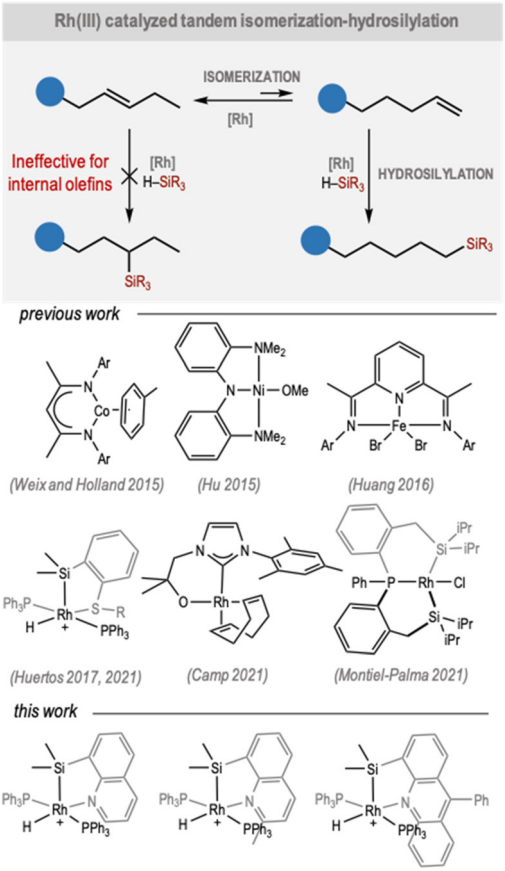

Fig. 1 Strategy for the rhodium-catalysed tandem isomerization–hydrosilylation reaction. Some catalysts reported to date and those used in this work.

neopentyl). The obtained results evidenced a clear dependence of the activity of the process on the size of the alkyl substituent on the sulfur atom. The best results were obtained when a catalyst containing bulky ^{i}Bu was used.[25]

Herein, and in order to further explore the tandem isomerization–hydrosilylation reaction, we reported the synthesis, full characterization (including X-ray) and catalytic activities of three new cationic and three new unsaturated hydrido-silyl-rhodium(III) complexes using bidentate silicon-based ligands derived from quinoline and acridine.

Results and discussion

Synthesis of ligands and complexes

Ligands employed in this work, 8-(dimethylsilyl)quinoline (**L1**),[30] 8-(dimethylsilyl)-2-methylquinoline (**L2**) and 4-(dimethylsilyl)-9-phenylacridine (**L3**), were synthesized by the reaction of bromide precursors with n-buthyllithium at −78 °C in THF, and subsequent addition of one equivalent of dimethylchlorosilane (Scheme 1). These compounds were characterized by ^{1}H and ^{13}C{^{1}H} NMR analyses. Moreover, bidimensional HMBC ^{1}H–^{29}Si experiments were performed to

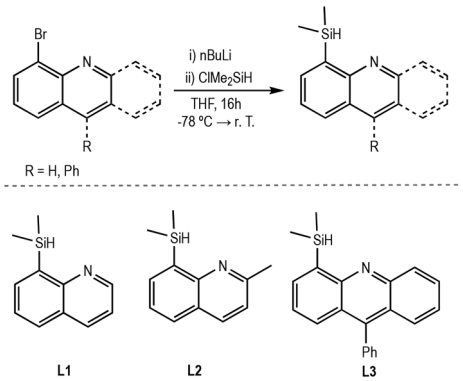

Scheme 1 Synthesis of pro-ligands used in this work (**L1**, **L2** and **L3**).

obtain the ^{29}Si chemical shift. As expected, the ^{1}H NMR spectra show a 1 H septuplet signal at 4.79 ppm for **L1**, 4.71 ppm for **L2**, 4.84 ppm for **L3** and a relative integral 6 H doublet (0.52 ppm for **L1**, 0.50 ppm for **L2**, 0.63 ppm for **L3**) that corresponds to Si–H and $Si(CH_3)_2$, respectively. Compound **L2** exhibits a 3 H singlet signal at 2.75 ppm for the methyl at position 2 of the quinoline. The ^{1}H–^{29}Si HMBC NMR spectra of these compounds confirm the presence of a silicon atom in their structures showing the correlation between the signal assigned to the methyl groups and the silicon atom of the $Si(CH_3)_2$ fragment (^{29}Si = −18.5 ppm for **L1**; −17.7 ppm for **L2**; −16.6 ppm for **L3**). Notice that the ^{29}Si NMR chemical shift found is characteristic of dimethyl-aryl-hydrosilanes [*e.g.* ^{29}Si ($PhMe_2SiH$) = −17.6 ppm].[31]

The addition of compounds **L1–L3** to $[RhCl(PPh_3)_3]$ in dichloromethane at room temperature led to the formation of neutral 16-electron Rh(III) complexes $[RhCl(H)(L)PPh_3]$ (**1-L1**, **1-L2** and **1-L3**) (Scheme 2). Complexes **1-L1**, **1-L2** and **1-L3** were characterized in solution by NMR spectroscopy and ESI-MS (electrospray ionization mass spectrometry), and in the solid state by elemental analysis. Complex **1-L2** was also characterized in the solid state by X-ray diffraction.

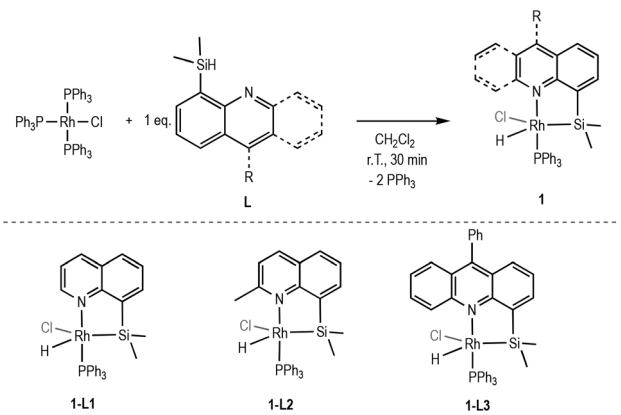

Scheme 2 Synthesis of neutral rhodium(III) complexes (**1-L1**, **1-L2** and **1-L3**).

In the ^{1}H NMR spectrum of **1-L1** a signal at $\delta = -17.23$ (dd, $J_{Rh-H} = 29$ Hz, $J_{P-H} = 21$ Hz) is assigned to the hydrido atom resulting from Si–H activation by the metal center. This signal is also indicative of the presence of a single phosphine coordinated to the metal center. Two other integral 3H methyl signals are observed at $\delta = -0.20$ and $\delta = 0.64$, which correlate with two resonances at $\delta = 4.1$ and $\delta = 7.7$ in the corresponding ^{13}C{^{1}H} NMR spectrum. These results are indicative of two non-equivalent $SiMe_2$ units. The ^{31}P{^{1}H} NMR spectrum shows a unique signal at $\delta = 50.7$ (d, $J_{Rh-P} = 149$ Hz). A ^{1}H–^{29}Si HMBC experiment was used to obtain the chemical shift of the silicon atom ($\delta = 41.2$), which supports Si–H activation by the metal center and the formation of a Rh(III) complex.[32–34]

The NMR characterization of compounds **1-L2** and **1-L3** is analogous to that of **1-L1** (more details are provided in the ESI†), indicating that they are isostructural complexes.

Complex **1-L2** was also characterized by single-crystal X-ray structural determination (Fig. 2). The coordination geometry of the Rh(III) atom is distorted trigonal bipyramidal. The apical positions are located at the phosphorus atom of the triphenylphosphine (P1) and the nitrogen atom (N1) of the bidentate ligand **L2** and the equatorial plane is occupied by the chloride ion (Cl1), hydrido atom (H1) and the silicon atom of the bidentate ligand Si1. The sum of the three angles Cl1–Rh1–H1, H1–Rh1–Si1 and Si1–Rh1–Cl1 is 359.1° and the N1–Rh1–P1 angle of 172.7° suggests this geometry. However, the angles of Si1–Rh1–Cl1 (122.4°), Si1–Rh1–H (67.5°) and Cl1–Rh1–H (169.2°) indicate a large distortion of this geometry. It is not surprising that by adopting this geometry, the silicon atom is placed in an equatorial position due to its *trans* influence.

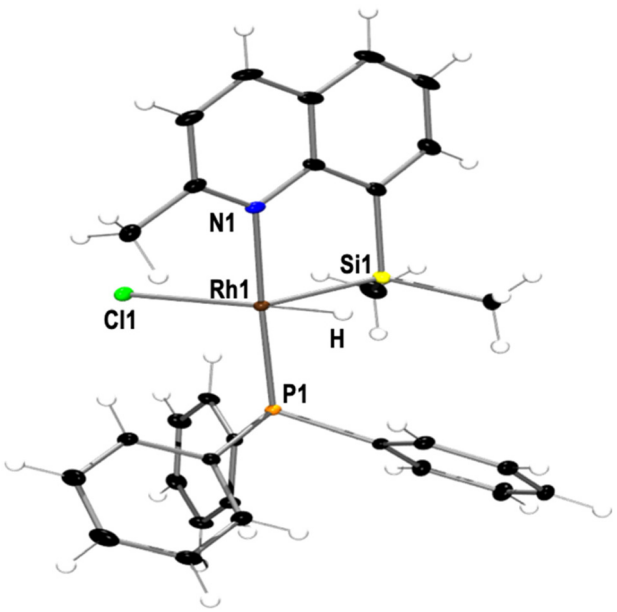

Fig. 2 Molecular structure of **1-L2**. Displacement of ellipsoids are drawn at 50% of probability. Selected bond lengths [Å] and angles [°]: Rh1–Cl1 2.4141(6), Rh1–Si1 2.2635(7), Rh1–P1 2.2393(6), Rh1–N1 2.1351 (2); N1–Rh1–P1 172.74(6), Si1–Rh1–Cl1 122.41(2).

We decided to synthesize cationic complexes similar to those previously reported, [Rh(H){$SiMe_2$(*o*-C_6H_4SR)}(PPh_3)$_2$][BAr^F_4] (R = Me, iBu, Pe, Bn, ^{neo}Pe),[24,25] which proved to be highly efficient as homogeneous catalysts in the isomerization–hydrosilylation tandem reaction.

As shown in Scheme 3, the treatment of [RhCl(PPh_3)$_3$] with **L1–L3** and an equimolar amount of Na[BAr^F_4] in CH_2Cl_2 at room temperature yielded Rh(III) 16-electron cationic complexes [Rh(H){(**L**)}(PPh_3)$_2$][BAr^F_4] (**2-L1**, **2-L2** and **2-L3**). These complexes were characterized by conventional spectroscopic and analytical methods, as well as by X-ray crystallography, in the case of **2-L2**.

The ^{1}H NMR spectra of all compounds show a doublet of triplets at around −12 ppm (**2-L1**, $\delta = -12.41$, $J_{Rh-H} = 17$ Hz, $J_{P-H} = 13$ Hz; **2-L2**, $\delta = -12.48$, $J_{Rh-H} = 16$ Hz, $J_{P-H} = 13$ Hz; **2-L3**, $\delta = -12.07$, $J_{Rh-H} = 17$ Hz, $J_{P-H} = 12$ Hz) assigned to the rhodium hydride originating from the oxidative addition of hydrosilanes to the metal center. Also, in the ^{1}H NMR spectra the 6H singlet signals at $\delta = 0.23$ for **2-L1**, $\delta = 0.18$ for **2-L2** and $\delta = 0.24$ for **2-L3** are assigned to the $SiMe_2$ unit. The ^{31}P{^{1}H} NMR spectra show a unique doublet signal (**2-L1**, $\delta = 43.8$, $J_{Rh-P} = 121$ Hz; **2-L2**, $\delta = 43.1$, $J_{Rh-P} = 123$ Hz; **2-L3**, $\delta = 45.0$, $J_{Rh-P} = 123$ Hz) that indicates equivalent triphenylphosphine groups. As for neutral complexes, ^{1}H–^{29}Si HMBC experiments were used to obtain the chemical shift of the silicon atom (**2-L1**, $\delta = 56.3$; **2-L2**, $\delta = 58.9$; **2-L3**, $\delta = 58.4$) and support Si–H activation by the metal center.

The similarity of the spectroscopic data suggests that cationic complexes **2-L1**, **2-L2** and **2-L3** are isostructural. Moreover, these data also suggest a square pyramidal structure for the cation of these complexes, with a strong σ-donor silyl fragment *trans* to the vacant octahedral site, as was already proposed for the related compounds [Rh(H){$SiMe_2$(*o*-C_6H_4SR)}(PPh_3)$_2$][BAr^F_4].[24,25] This structural description, based on NMR characterization studies in solution, was confirmed by the solid-state structure determination of compound **2-L2** (Fig. 3). In the solid state, the formal Rh(III) center adopts a square pyramidal geometry where the base of the pyramid is occupied by the hydrido atom (H1), the two phosphines placed in a *trans*

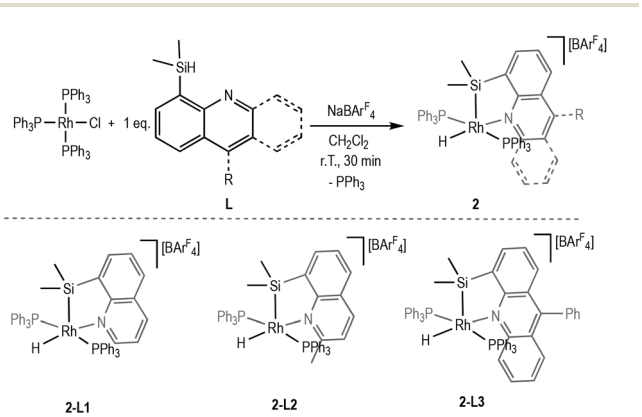

Scheme 3 Synthesis of cationic rhodium(III) complexes (**2-L1**, **2-L2** and **2-L3**).

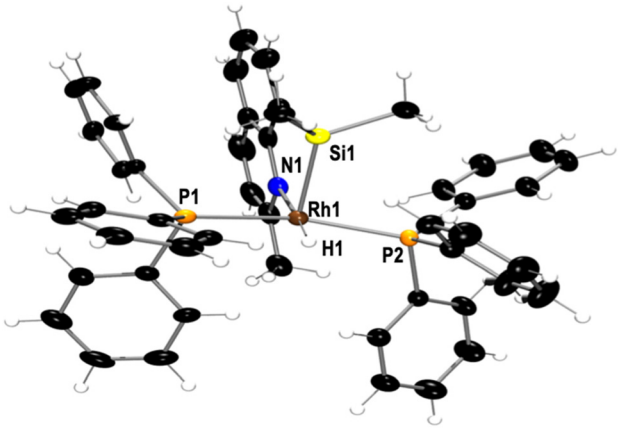

Fig. 3 Molecular structure of **2-L2**. The anion is omitted for clarity. Displacement of ellipsoids are drawn at 50% of probability. Selected bond lengths [Å] and angles [°]: Rh1–Si1 2.2985(9), Rh1–P1 2.3039(19), Rh1–P2 2.3388(10), Rh1–N1 2.171(2); N1–Rh1–P1 104.87(11), P2–Rh1–N1 93.41(7).

position to each other and the nitrogen atom (N1) from the bidentate ligand **L2**. The *trans* position of the phosphines creates a plane of symmetry, which is in good agreement with the data observed in solution. The apical position of the pyramid is located at the silicon atom of **L2** (Si1). The coordinative vacancy *trans* to the silyl fragment is consistent with the *trans* influence of the silyl fragment.

Catalytic isomerization–hydrosilylation of alkenes

As noted in the introduction, similar rhodium complexes proved to be effective catalysts for the tandem isomerization–hydrosilylation reaction, converting remote alkenes into terminal silanes.[24,25] With this in mind, the new neutral (**1-L**) and cationic (**2-L**) rhodium complexes have been tested as precatalysts in the aforementioned reaction.

The activity of these new rhodium(III) complexes was initially tested in the hydrosilylation of 1-hexene with an equimolar amount of Et_3SiH and 0.5 mol% loading of the corresponding catalyst (**1-L1**, **1-L2**, **1-L3**, **2-L1**, **2-L2** or **2-L3**).

The catalytic reaction was carried out at room temperature, under an N_2 atmosphere, and in the absence of solvent. The conversions were estimated by ^{1}H NMR analysis after 16 hours of reaction progress (Table 1). Neutral complexes (**1-L1**, **1-L2** and **1-L3**) were found to be inactive for this reaction (Table 1, entries 1–3), with the 1-hexene remaining unreacted. It should be noted that 1-hexene was not isomerized.

In contrast to this, we were pleased to observe that the cationic complexes (**2-L1**, **2-L2** and **2-L3**) were active under these reaction conditions and based on the ^{1}H NMR spectra of the crude reaction products (Fig. S4–S6 in the ESI†), 1-hexene gave selectively the linear hexyltriethylsilane (Table 1, entries 4–6). Complexes **2-L2** and **2-L3**, which have a substituent in the *ortho* position of the pyridine ring, were found to be more active catalysts than **2-L1**, with **2-L2** being the most active from the series (94% conversion, Table 1, entry 5). Analysis of the

Table 1 Hydrosilylation of 1-hexene with Et_3SiH using rhodium(III) catalysts[a]

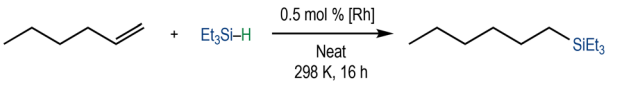

Entry	Catalyst	Yield[b]
1	**1-L1**	—
2	**1-L2**	—
3	**1-L3**	—
4	**2-L1**	85%
5	**2-L2**	94%
6	**2-L3**	87%

[a] Reaction conditions: alkene (0.25 mmol), Et_3SiH (0.25 mmol), catalyst 0.5 mol%, solvent-free, at room temperature. [b] Yields calculated based on ^{1}H NMR ($CDCl_3$) analysis using dichloroethane (0.125 mmol) as internal standard.

^{1}H NMR spectra of the reaction mixtures showed that with cationic rhodium complexes, the unreacted 1-hexene has isomerized to internal hexenes.

The cationic derivatives were tested in the tandem isomerization–hydrosilylation of a more challenging substrate, *trans*-3-hexene, under the standard reaction conditions (Table 2, entries 1–3). These reactions were analyzed by ^{1}H NMR after 16 hours, showing that the only silylated product formed was also hexyltriethylsilane (Fig. S7–S9 in the ESI†), confirming that the reaction occurred through a tandem isomerization–hydrosilylation process. Also in this case, complex **2-L2** was the most active catalyst from the series, while **2-L3** outperforms **2-L1** (Table 2 and Fig. S7–S9 in ESI†). This reaction was also performed using different solvents, CD_2Cl_2 and THF-d_8 (Table 2, entries 4 and 5), and the results show lower conversions. In both cases the lower conversion could be explained by the lower concentration of the reaction mixture. In addition, when using THF-d_8, coordination of the solvent to the metal center should be considered.

Considering the structure of our precatalysts and the previous studies performed by the group,[25] it is reasonable to con-

Table 2 Hydrosilylation of *trans*-3-hexene with Et_3SiH using **2-L1**–**2-L3** catalysts[a]

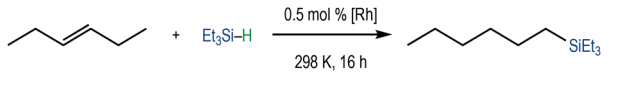

Entry	Catalyst	Solvent	Yield[b]
1	**2-L1**	Neat	45%
2	**2-L2**	Neat	70%
3	**2-L3**	Neat	65%
4[c]	**2-L2**	CD_2Cl_2	48%
5[c]	**2-L2**	THF-d_8	17%

[a] Reaction conditions: alkene (0.25 mmol), Et_3SiH (0.25 mmol), catalyst 0.5 mol%, solvent-free, at room temperature. [b] Yields calculated based on ^{1}H NMR ($CDCl_3$) analysis using dichloroethane (0.125 mmol) as internal standard. [c] 1 mL of solvent (alkene concentration 0.25 M).

sider a hydride mechanism for the isomerization process[35,36] and a σ-bond metathesis for the anti-Markovnikov hydrosilylation[37,38] (see the ESI† for more details). The trigonal bipyramidal geometry of the neutral complexes could be considered responsible for the lack of catalytic activity of these systems. In contrast, the cationic complexes have a coordinative vacancy in the *cis* position of the hydride, an ideal situation for isomerization reactions (and subsequent hydrosilylation) to occur. As mentioned above, similar cationic Rh(III) complexes $[Rh(H)\{SiMe_2(o\text{-}C_6H_4SR)\}(PPh_3)_2][BAr^F{}_4]$ were studied previously in our group as catalysts for tandem alkene isomerization–hydrosilylation, showing that the size of the substituent on the sulfur atom was an important factor determining the catalytic activity, with the catalyst containing bulky ^{i}Bu being the most active one.[25] Moreover, we proposed that the rate of the entire process depends on the effectiveness of the isomerization reaction.[25,39] Based on these precedents, we have analyzed the catalytic pocket of the Rh(III) complexes to compare the steric hindrance of the Si,N ligands **L1** and **L2** upon coordination to the metal center. Cationic complexes **2-L1** and **2-L2** were studied using topographic steric maps (Fig. 4).[40] As in classical geographic physical maps, different colors are used to show the elevation of the ligands with respect to the zero level fixed in the rhodium atom. The triphenylphosphine ligands are located on the *y*-axis, north and south of the map. The western region is located at the hydrido atom, while the nitrogen atom is on the east of the map. Comparison of the steric maps of the complexes indicates some slight differences in the catalytic pocket. The more intense red area of **2-L2** and **2-L3** compared to that of **2-L1** in the eastern region agrees with a larger steric hindrance due to the *ortho* substitution at the aromatic ring. These data indicate that, as in previously published studies, the complex with the most bulky ligand is the most active for this catalytic reaction.[25] It could be proposed that isomerization of 1-hexene would be slightly favored in the case of catalysts with bulkier ligands. This would result in higher catalytic activity in the tandem process.

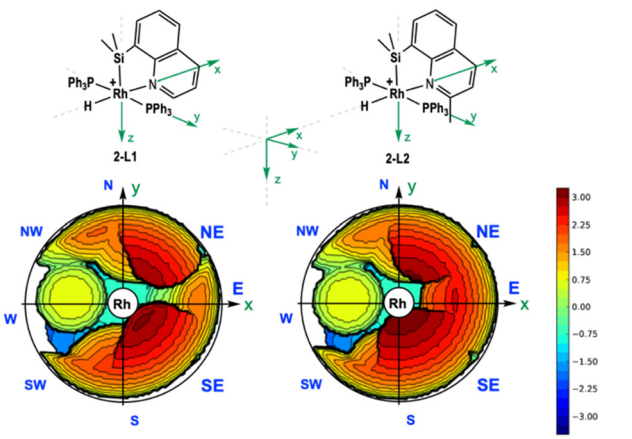

Fig. 4 Steric maps of **2-L1** and **2-L2**. The complexes are oriented according to the schemes above.

The good activity of complex **2-L2** in *trans*-3-hexene isomerization and hydrosilylation prompted us to extend this study to other internal olefins (Table 3). First, other hexene isomers (*trans*-2-hexene, *cis*-2-hexene and *cis*-3-hexene) were tested under our standard conditions. In all cases (Table 3, entries 1–3 and Fig. S10–S12 in the ESI†), the cationic Rh(III) complex **2-L2** catalyzes the tandem isomerization–hydrosilylation with complete selectivity to the formation of hexyltriethylsilane. The conversions obtained for different hexene isomers could be expected considering the proposed mechanism for isomerization. Since it is an equilibrium between the different alkene isomers, it is not strange that some of them are transformed into 1-hexene more efficiently. The catalytic isomerization–hydrosilylation of several internal octene isomers, including the most remote ones *trans*/*cis*-4-octene, had also been performed (Table 4, entries 4–8 and Fig. S13–S17 in the ESI†). Complex **2-L2** catalyzes these reactions with selectivity to the formation of triethyloctylsilane.

No reaction was observed using cyclooctene as a substrate (Table 3, entry 9). This confirms the selectivity of our catalytic

Table 3 Hydrosilylation of internal alkenes with Et_3SiH using the **2-L2** catalyst[a]

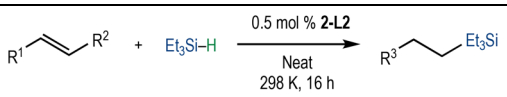

Entry	Alkene	Product/yield[b]
1	*trans*-2-hexene	76%
2	*cis*-2-hexene	60%
3	*cis*-3-hexene	51%
4	*trans*-2-octene	68%
5	*cis*-2-octene	61%
6	*trans*-3-octene	63%
7	*trans*-4-octene	63%
8	*cis*-4-octene	59%
9	cyclooctene	—

[a] Reaction conditions: alkene (0.25 mmol), Et_3SiH (0.25 mmol), catalyst 0.5 mol%, solvent-free, at room temperature. [b] Yields calculated based on ^1H NMR ($CDCl_3$) analysis using dichloroethane (0.125 mmol) as internal standard.

Table 4 Hydrosilylation of other alkenes with Et_3SiH using the **2-L2** catalyst[a]

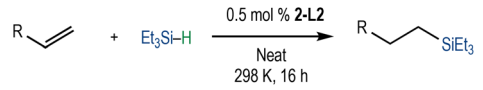

Entry	Alkene	Product/yield[b]
1	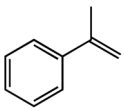	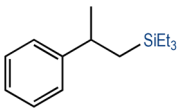
2	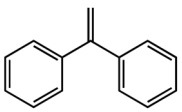	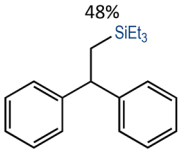 48%
3	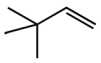	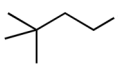 23%
4	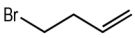	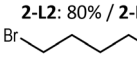 **2-L2**: 80% / **2-L1**: 78%
5	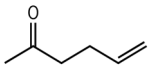	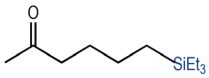 84% 65%

[a] Reaction conditions: alkene (0.25 mmol), Et_3SiH (0.25 mmol), catalyst 0.5 mol%, solvent-free, at room temperature. [b] Yields calculated based on ^1H NMR ($CDCl_3$) analysis using dichloroethane (0.125 mmol) as internal standard.

system for the hydrosilylation of terminal alkenes. The results obtained with these catalysts are distinct in terms of activity than those previously reported by the group based on Si–S chelating ligands. This suggests that weaker sulfur-coordination to the metal center has an influence on the catalytic activities of these compounds. This has previously been observed for hydrosilylation reactions.[41] However, this catalytic system shows quite good activity compared to others found in the literature, which require higher catalyst loadings or higher temperatures.[20–27]

To complete this study, the hydrosilylation of other alkenes with **2-L2** was studied (Table 4). First, unisomerizable terminal alkenes, such as α-methylstyrene, 1,1-diphenylethylene and *tert*-butylethylene (tbe), were tested under standard conditions. As expected, the selectivity towards the anti-Markovnikov product was complete (Table 4, entries 1–3 and Fig. S18–S20†). Low conversions were observed for styrene derivatives (48% conversion for α-methylstyrene and 23% conversion for 1,1-diphenylthylene), presumably due to the steric hindrance caused by the β-substitution of the terminal olefin. A good conversion to (3,3-dimethylbutyl)triethylsilane (80%) was achieved for tbe. Hydrosilylation of tbe was also performed using **2-L1** as a precatalyst giving a similar conversion value (Table 4, entry 3, Fig. S24†). This agrees with the isomerization being the rate-limiting process. To conclude this study, alkenes bearing additional functional groups were used (Table 4 entries 4 and 5 and Fig. S21 and S22 in the ESI†). The catalytic hydrosilylation of 4-bromo-2-butene under standard reaction conditions led to the formation of the desired terminal alkylsilane with good conversion and complete selectivity. Finally, when 5-hexen-2-one was used, hydrosilylation of the alkene was achieved with 65% selectivity, showing the preference of the system for the hydrosilylation of alkenes in preference to carbonyls.

Conclusions

A facile oxidative addition of the Si–H bond to the Wilkinson's catalyst has been used to synthesize three neutral and three cationic five-coordinate Rh(III) complexes bearing Si,N bidentate ligands [8-(dimethylsilyl)quinoline (**L1**), 8-(dimethylsilyl)-2-methylquinoline (**L2**) and 4-(dimethylsilyl)-9-phenylacridine (**L3**)]. The neutral complexes $[RhCl(H)(\mathbf{L})PPh_3]$ (**1-L1**, **1-L2** and **1-L3**) show a distorted trigonal bipyramid structure, while the cationic complexes $[Rh(H)(\mathbf{L})(PPh_3)_2][BAr^F{}_4]$ (**2-L1**, **2-L2** and **2-L3**) present a square pyramidal structure. The 6 complexes were tested as catalysts in the 1-hexene hydrosilylation reaction, being active only for the cationic complexes. These cationic Rh(III) complexes, **2-L1**, **2-L2** and **2-L3**, are also efficient catalysts for the more challenging tandem isomerization–hydrosilylation reaction, forming terminal silanes from remote alkenes. Of the three cationic complexes, the most active catalyst was **2-L2**. This result is in agreement with our previous studies using analogous cationic Rh(III) complexes $[Rh(H)\{SiMe_2(o\text{-}C_6H_4SR)\}(PPh_3)_2][BAr^F{}_4]$ (R = Me, ^{i}Bu), which showed that a larger steric hindrance in the catalytic pocket results in a higher catalytic activity of the complex.

Conflicts of interest

There are no conflicts to declare.

Acknowledgements

This publication is part of the projects PID2019-111281GB-I00 funded by MCIN/AEI/10.13039/501100011033 and IT1741-22 and IT1553-22 founded by Gobierno Vasco. The authors thank SGiker for technical and human support. Universidad del País Vasco (UPV/EHU) (to U. P.) and IKERBASQUE (to M. H. and Z. F.) are acknowledged for personnel funding.

References

1 I. Flemin, in *Comprehensive Organic Chemistry II*, ed. D. Burton and W. D. Ollis, Pergamon Press, Oxford, UK, 1979, p. 577.
2 B. Marciniec, *Applied Homogeneus Catalysis with Organometallic Compounds*, Weinheim, Germany, 1996.

3 D. R. Thomas, in *Comprehensive Organometallic Chemistry*, ed. W. W. Abel, F. G. A. Stone and G. Wilkinson, Pergamon Press, Oxford, UK, 1995, p. 114.
4 J. L. Speier, in *Advances in Organometallic Chemistry*, ed. F. G. A. Stone and W. Robert, Academic Press, 1979, vol. 17, p. 407.
5 J. L. Speier, J. A. Webster and G. H. Barnes, *J. Am. Chem. Soc.*, 1957, **79**, 974–979.
6 P. B. Hitchcock, M. F. Lappert and N. J. W. Warhurst, *Angew. Chem., Int. Ed. Engl.*, 1991, **30**, 438–440.
7 A. M. Schroeder and S. M. Wrighton, *J. Organomet. Chem.*, 1977, **128**, 345–358.
8 N. J. Archer, R. N. Haszeldine and R. V. Parish, *J. Chem. Soc., Dalton Trans.*, 1979, 695–702.
9 M. Brookhart and B. E. Grant, *J. Am. Chem. Soc.*, 1993, **115**, 2151–2156.
10 J. F. Harrod and A. H. Chalk, *J. Am. Chem. Soc.*, 1965, **87**, 1133.
11 F. Kakiuchi, Y. Tanaka, N. Chatani and S. Murai, *J. Organomet. Chem.*, 1993, **456**, 45–47.
12 Z. Mo, J. Xiao, Y. Gao and L. Deng, *J. Am. Chem. Soc.*, 2014, **136**, 17414–17417.
13 C. L. Reichel and M. S. Wrighton, *Inorg. Chem.*, 1980, **19**, 3858–3860.
14 F. Seitz and M. S. Wrighton, *Angew. Chem., Int. Ed. Engl.*, 1988, **27**, 289–291.
15 L. Yong, K. Kirleis and H. Butenschön, *Adv. Synth. Catal.*, 2006, **348**, 833–836.
16 P. Jiajian, B. Ying, L. Jiayun and L. Guoqiao, *Curr. Org. Chem.*, 2011, **15**, 2802–2815.
17 S. C. Bart, E. Lobkovsky and P. J. Chirik, *J. Am. Chem. Soc.*, 2004, **126**, 13794–13807.
18 A. M. Tondreau, C. C. H. Atienza, K. J. Weller, S. A. Nye, K. M. Lewis, J. G. P. Delis and P. J. Chirik, *Science*, 2012, **335**, 567–570.
19 J. Y. Wu, B. N. Stanzl and T. Ritter, *J. Am. Chem. Soc.*, 2010, **132**, 13214–13216.
20 D. Peng, Y. Zhang, X. Du, L. Zhang, X. Leng, M. D. Walter and Z. Huang, *J. Am. Chem. Soc.*, 2013, **135**, 19154–19166.
21 C. Chen, M. B. Hecht, A. Kavara, W. W. Brennessel, B. Q. Mercado, D. J. Weix and P. L. Holland, *J. Am. Chem. Soc.*, 2015, **137**, 13244–13247.
22 I. Buslov, J. Becouse, S. Mazza, M. Montandon-Clerc and X. Hu, *Angew. Chem., Int. Ed.*, 2015, **54**, 14523–14526.
23 X. Jia and Z. Huang, *Nat. Chem.*, 2016, **8**, 157–161.
24 S. Azpeitia, M. A. Garralda and M. A. Huertos, *ChemCatChem*, 2017, **9**, 1901–1905.
25 U. Prieto, S. Azpeitia, E. San Sebastian, Z. Freixa, M. A. Garralda and M. A. Huertos, *ChemCatChem*, 2021, **13**, 1403–1409.
26 R. Srivastava, M. Jakoobi, C. Thieuleux, E. A. Quadrelli and C. Camp, *Dalton Trans.*, 2021, **50**, 869–879.
27 N. S. Abeynayake, J. Zamora-Moreno, S. Gorla, B. Donnadieu, M. A. Muñoz-Hernández and V. Montiel-Palma, *Dalton Trans.*, 2021, **50**, 11783–11792.
28 A. J. Chalk, *J. Organomet. Chem.*, 1970, **21**, 207–213.
29 A. J. Chalk and J. F. Harrod, *J. Am. Chem. Soc.*, 1965, **87**, 16–21.
30 P. I. Djurovich, A. Safir, N. Keder and R. J. Watts, *Coord. Chem. Rev.*, 1991, **111**, 201–214.
31 C. R. Ernst, L. Spialter, G. R. Buell and D. L. Wilhite, *J. Am. Chem. Soc.*, 1974, **96**, 5375–5381.
32 S. Azpeitia, B. Fernandez, M. A. Garralda and M. A. Huertos, *Eur. J. Inorg. Chem.*, 2015, 5451–5456.
33 N. Almenara, J. I. Miranda, A. Rodriguez-Dieguez, M. A. Garralda and M. A. Huertos, *Dalton Trans.*, 2019, **48**, 17179–17183.
34 T. Komuro, D. Mochizuki, H. Hashimoto and H. Tobita, *Dalton Trans.*, 2022, **51**, 9983–9987.
35 E. Larinov, H. Li and C. Mazet, *Chem. Commun.*, 2014, **50**, 9816–9526.
36 S. M. M. Knapp, S. E. Shaner, D. Kim, D. Y. Shopov, J. A. Tendler, D. M. Pudalov and A. R. Chianese, *Organometallics*, 2014, **33**, 473–484.
37 M. Brookhart and B. E. Grant, *J. Am. Chem. Soc.*, 1993, **115**, 2151–2156.
38 R. N. Perutz and S. Sabo-Etienne, *Angew. Chem., Int. Ed.*, 2007, **46**, 2578–2592.
39 J. V. Obligación and P. J. Chirick, *J. Am. Chem. Soc.*, 2013, **135**, 19107–19110.
40 L. Falvine, Z. Cao, A. Petta, L. Serra, A. Poater, R. Oliva, V. Scarano and L. Cavallo, *Nat. Chem.*, 2019, **11**, 872–879.
41 M. Konkol, M. Kondracka, P. Voth, T. P. Spaniol and J. Okuda, *Organometallics*, 2008, **27**, 3774–3784.